

1 Support vector regression integrated with fruit fly optimization algorithm 2 for river flow forecasting in Lake Urmia basin

3 Saeed Samadianfard¹, Salar Jarhan², Ely Salwana³, Amir Mosavi^{4,5,6}, Shahaboddin Shamshirband^{7,8*}

4 ¹ Department of Water Engineering, Faculty of Agriculture, University of Tabriz, Tabriz, Iran

5 ² Department of Hydrosocieties, Technische Universität Dresden, Dresden, Germany

6 ⁴ Centre for Accident Research Road Safety-Queensland, Queensland University of Technology, Brisbane QLD 4059,
7 Australia;

8 ⁵ School of the Built Environment, Oxford Brookes University, Oxford OX3 0BP, UK

9 ⁶ Institute of Automation, Kando Kalman Faculty of Electrical Engineering, Obuda University, Budapest 1034,
10 Hungary

11 ⁷ Department for Management of Science and Technology Development, Ton Duc Thang University, Ho Chi Minh
12 City, Viet Nam

13 ⁸ Faculty of Information Technology, Ton Duc Thang University, Ho Chi Minh City, Viet Nam

14

15

16

17 Abstract

18 Adequate knowledge about the development and operation of the components of water systems is of high
19 importance in order to optimize them. For this reason, forecasting of future events becomes greatly significant
20 due to making the appropriate decision. Moreover, operational river management severely depends on accurate
21 and reliable flow forecasts. In this regard, current study inspects the accuracy of support vector regression
22 (SVR), and SVR regulated with fruit fly optimization algorithm (FOASVR) and M5 model tree (M5), in river
23 flow forecasting. Monthly data of river flow in two stations of the Lake Urmia Basin (Vaniar and Babarud
24 stations on the Aji Chay and the Barandouz Rivers) were utilized in the current research. Additionally, the
25 influence of periodicity (π) on the forecasting enactment was examined. To assess the performance of
26 mentioned models, different statistical meters were implemented, including root mean squared error (RMSE),
27 mean absolute error (MAE), correlation coefficient (R), and Bayesian information criterion (BIC). Results
28 showed that the FOASVR with RMSE (4.36 and 6.33 m³/s), MAE (2.40 and 3.71 m³/s) and R (0.82 and 0.81)
29 values had the best performances in forecasting river flows in Babarud and Vaniar stations, respectively. Also,
30 regarding BIC parameters, Q_{t-1} and π were selected as parsimonious inputs for predicting river flow one month
31 ahead. Overall findings indicated that, although both FOASVR and M5 predicted the river flows in suitable
32 accordance with observed river flows, the performance of FOASVR was moderately better than the M5 and
33 periodicity noticeably increased the performances of the models; consequently, FOASVR can be suggested as
34 the accurate method for forecasting river flows.

35 **Keywords:** River flow forecasting; Optimization; M5 model tree; Support vector regression; Fruit fly
36 optimization algorithm

37

38

39 **1. Introduction**

40 Dependable approximation of discharge is imperative in water resources management (Onyari and Ilunga,
41 2010). Nowadays, stream flow predicting is a dynamic and active research zone which has been studied. The
42 stream flow is censorious to numerous actions such as planning and designing flood protections for farming
43 lands and urban areas, and evaluating the amount allowable extracted water from a river for irrigation (Ismail
44 et al., 2010). By happening a dynamic climate change and continues altering of environmental situations,
45 instantaneous approaches based on utilizing real past data rather than the hydrology of the catchments has
46 become more applicable (Fernando et al., 2012).

47 Generally, data mining is an influential novel methodology based on the abstraction of concealed information
48 from huge data. These tools forecast forthcoming movements of a special system using knowledge-driven
49 decisions resulted from enormous input-output data. M5 model tree (M5), as a sub-technique of data mining,
50 constructs tree based linear models for continues data. Lately, the implementation of M5, as decision tree based
51 regression method, have been stated for hydrological and water-related studies (Bhattacharya and Solomatine,
52 2005, 2006; Khan and See, 2006; Siek and Solomatine, 2007; Stravs and Brilly, 2007; Samadianfard et al.,
53 2014(a,b); Esmailzadeh et al. 2017). Londhe and Dixit (2011) implemented M5 to estimate river flow at two
54 stations of India. The models were established by the preceding values of gauged river flow and rainfall for
55 predicting river flow one day beforehand. Sattari et al., (2013) inspected the proficiencies of support vector
56 machine (SVM) and M5 model tree in forecasting flows of Sohu River. They revealed that M5 provided precise
57 predictions comparing with SVM.

58 SVM is a technique in which the strong points of traditional statistical methods, which are theory-oriented and
59 analytically simple, are utilized. SVM approach has been frequently implemented in the areas of hydrology
60 and forecasting time series. Liong and Sivapragasam (2002) applied the method for foreseeing floods. Yu et
61 al. (2004) suggested a method for forecasting daily runoff through combining Chaos Theory and the SVM
62 method. Recently, support vector regression (SVR) method has been developed based on SVM and shows
63 superiority in the prediction of hydrologic processes. Kalteh (2013) with applying Artificial Neural Network

64 (ANN) and SVR to monthly streamflow recorded in 2 different stations revealed that both models coupled
 65 with wavelet transformation produced more accurate outcomes than the regular models. Also, the results
 66 specified that SVR models had enhanced performances comparing ANN models. Wu et al. (2008) used a
 67 genetic algorithm to optimize the SVR model, and result exhibited that the suggested model could anticipate
 68 river flow precisely in comparison with other models. Londhe and Gavraskar (2015) utilized the SVR model
 69 to one-day ahead forecast river flow in two studied locations. The model results were favorable according to
 70 the low values of the evaluating metrics.

71 On the other hand, Cao and Wu (2016) coupled Fruit Fly Optimization algorithm (FOA) with SVR (named
 72 FOASVR) for optimizing the parameters of SVR. The obtained results exhibited that applying FOASVR had
 73 a significant role in increasing the prediction accuracy. Lijuan and Guohua (2016) used FOASVR which
 74 hybridizes the SVR model with FOA to estimate monthly incoming tourist flow. It was reported that the
 75 suggested FOASVR is a viable option for touristic applications.

76 The key objective of this research is exploiting the accuracy of M5, support vector regression, and optimized
 77 SVR with FOA for river flow forecasting in the Vaniar and Babarud stations on the Aji Chay and the
 78 Barandouz rivers, respectively, located in the Lake Urmia basin of Iran. Some evaluation parameters for error
 79 estimation are utilized for assessing the enactment of the considered models. To the best knowledge of the
 80 authors, FOA has not been integrated with SVR in river flow forecasting.

81

82 **2. Techniques applied in modeling**

83 **2.1 M5 model tree**

84 With a constant value at their leaves, model trees are based on regression trees (Witten and Frank, 2005). In
 85 this regard, M5, as one of the versions of model trees, has a high capability to forecast continuous numerical
 86 attributes (Quinlan, 1992). Moreover, two different steps are necessary to develop tree models. Firstly, a
 87 splitting principle should utilize for creating a decision tree. This criterion is constructed using the standard
 88 deviation (SD) of the class values which reach a node as a size of the error. So, the standard deviation reduction
 89 (SDR) is given by:

$$SDR = SD(T) - \sum \frac{|T_i|}{|T|} \times SD(T_i) \quad (1)$$

90 Where T is a set of data that reaches the node and T_i is the i^{th} subset of data. After the first step, data in the
 91 secondary nodes have lower SD comparing with initial nodes, so, M5 selects the split which expects to
 92 maximize error reduction. Producing a large tree is the main drawback of this step which may cause overfitting
 93 problem. Pruning techniques should be employed in order to fix this problem and avoid overfitting. Therefore,
 94 the second step for developing M5 involves these techniques and substitution of subtrees with LR functions.
 95 As a result, by applying these two steps, M5 develops an LR model for each subspace.

96

97 2.2 Support vector regression (SVR)

98 SVM is recognized as a technique for classification and regression (Vapnik, 1995). Generally, regression-
 99 based SVM is called SVR. For solving complex problems effectively, SVR is constructed based on minimizing
 100 the structural risk. So, insensitive loss function (ε -) identified as the model tolerating errors up to ε in the
 101 training data. Thus, the SVR pursues a linear function as follows:

$$F(x) = w^T x + b \quad (2)$$

102 Where w and b represent the coefficients of the weight vector. This can be clarified as the following problem:

$$\text{Min } \frac{1}{2} \|w\|^2 + C \sum_{i=1}^N (\xi_i + \xi_i^*) \quad \text{Subject to } \begin{cases} F(x) - y_i \leq \varepsilon + \xi_i^* \\ y_i - F(x) \leq \varepsilon + \xi_i \\ \xi_i, \xi_i^* \geq 0, \quad i = 1, 2, \dots, N \end{cases} \quad (3)$$

103 Where $C > 0$ is a penalty parameter which has to be selected earlier. The constant C can grade the experimental
 104 error. Moreover, ξ_i and ξ_i^* which are known as slack variables indicating the distance between real values and
 105 the corresponding boundary values of ε -tube. Hence, in order to minimize Eq. (2) subject to Eq. (3), the
 106 R function is given by (Gunn, 1998; Cimen, 2008):

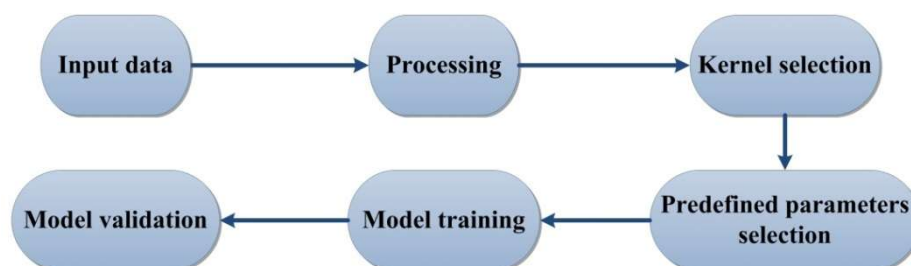
$$f(x) = \sum_{i=1}^N (\alpha_i^* - \alpha_i) K(x, x_i) + B \quad (4)$$

107 Where $K(x, x_i)$ is the Kernel function, $\alpha_i, \alpha_i^* \geq 0$ are the Lagrange multipliers and B is a bias term. Kernel trick
 108 is an approach which is used to solve this problem by SVR (Smola and Scholkopf, 2004). In this study, the
 109 widely implemented kernel named radial basis function (RBF) is utilized for building optimum SVR model.
 110 Converging fast, working well in high dimensional spaces and being simple are some advantages of the
 111 selected kernel (Wu et al., 2009).

$$k(x, x_i) = \exp(-\gamma \|x - x_i\|^2) \quad (5)$$

112 Where γ is the bandwidth of kernel function. C , γ and ε are three predefined parameters. In this research, 1,
 113 0.01, and 0.001 were selected as default amounts which are used in WEKA software, respectively. Fig. 1
 114 indicates schematic configuration of SVthe R model.

115



116

117

Fig. 1 schematic configuration of SVR model.

118

119 2.3. Fruit fly Optimization Algorithm (FOA)

120 FOA which was introduced by Pan (2012) is a swarm intelligent optimization algorithm that imitates the
 121 activities of fruit flies for searching the global optimum. Fruit flies can identify the smell from even 40
 122 kilometers and fly on the way to it. Fig. 2 displays the food searching progression utilized by fruit fly
 123 iteratively. According to Pan (2012), the following equations are exploited to acquire the initial swarm location
 124 of a fruit fly:

$$X_0 = rand(LR) \quad (6)$$

$$Y_0 = rand(LR)$$

125 Where LR is the location range of the accidental, initial fruit fly swarm. Subsequently, unexpected search
 126 direction and distance for foraging of the fruit flies are given by:

$$X_i = X_0 + rand(FR) \quad (7)$$

$$Y_i = Y_0 + rand(FR)$$

127 where FR is the random flight range, so, smell concentration judgment value (S) can be computed by:

$$S_i = 1/\sqrt{x_i^2 + y_i^2} \quad (8)$$

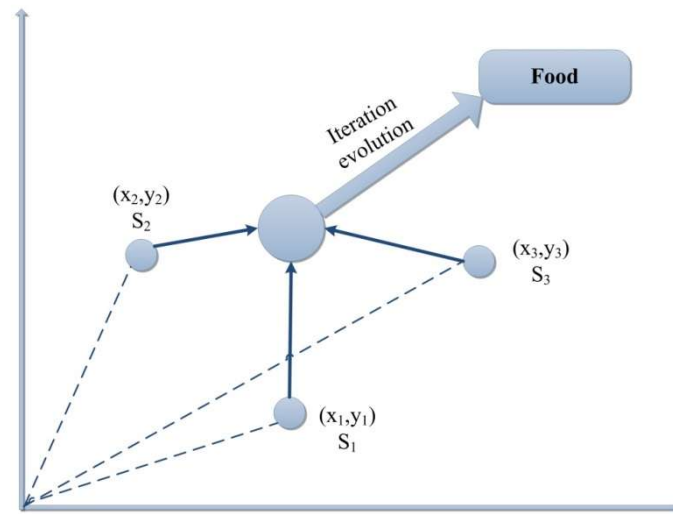


Fig. 2 food searching process utilized by fruit fly iteratively.

128

129

130 For improving the performance of river flow forecasting, FOA was implemented for choosing optimized values
 131 of three SVR parameters including c , ε , γ , which are connected to $(S_{ci}, S_{\varepsilon i}, S_{\gamma i})$ (i.e., $C = S_{ci}$, $\gamma = S_{\gamma i}$, and $\varepsilon =$
 132 $S_{\varepsilon i}$). The flowchart of the mentioned procedure (FOASVR) is displayed in Fig. 3. Moreover, the differences
 133 among the predicted and the actual values were evaluated by mean squared error (MSE), as presented in
 134 equation below:

$$MSE = \frac{\sum_{i=1}^n (p_i - o_i)^2}{n} \quad (9)$$

135 where p_i and o_i are the i^{th} predicted and observed values and n is the entire number of data. The fruit fly saves
 136 the finest smell concentration value and the corresponding coordinate among the swarms, then flies towards
 137 the next place. When the new result is not superior to the previous iteration or the iteration number reaches its
 138 maximum, or the error of the prediction reaches the predefined value, this process will stop. Therefore, optimal
 139 values are acquired, and the model has the best performance with these values.

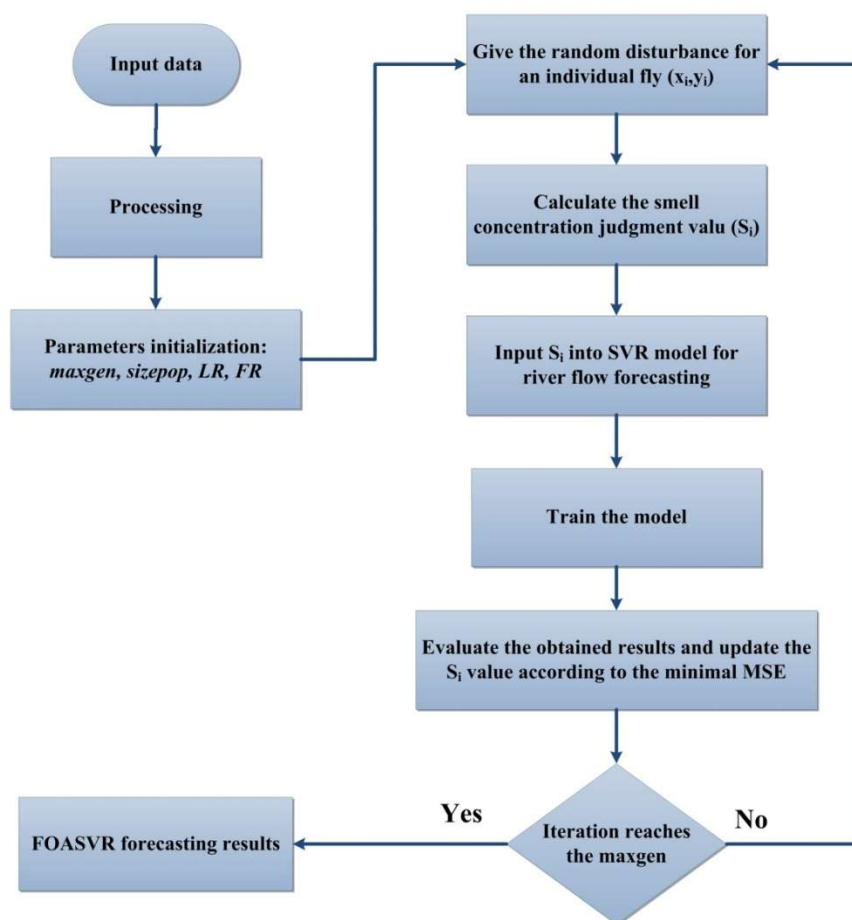


Fig. 3 The FOASVR flowchart

140

141

142 In this research, data were normalized to be between 0 and one because it helps to increase the accuracy of the
 143 model and to predict performance (Chang and Lin, 2001). Besides, LR and FR were chosen to be included [0,
 144 10] and [-1, 1], respectively; Also, the maximum iteration number (maxgen) was equal to 100, and the
 145 population size (size pop) was selected to be 20 in order to have reasonable efficiency. Moreover, Libsvm
 146 toolbox was used to run SVR in this article.

147 3. Study area

148 In the current study, the monthly river flow was used for the Vaniar station on the Aji Chay Stream and the
 149 Babarud station on the Barandouz River, both located at Lake Urmia basin of Iran (Fig. 4). The observed data
 150 include 780 monthly river flows (65 years from 1952 to 2017) for Babarud station and 744 monthly records
 151 (62 years from 1952 to 2014) for Vaniar station. Moreover, there is no basic and technical way of separating
 152 training and testing data. For example, the study of Kurup and Dudani (2002) used a total of their 63% of data
 153 for model development whereas Pal (2006) used 69%, and Samadianfard et al. (2013, 2014) used 67% of total
 154 data, and Deo et al. (2018) and Samadianfard et al. (2018) used 70% of total data to develop their models.

155 Thus, for developing the studied models, the data are divided into training (70%) and testing (30%).
 156 Additionally, Table 1 displays the statistics of implemented data for both stations. The observed data confirms
 157 high positive values of skewness ($C_{sx} = 2.13$ and 3.19). Furthermore, the low auto-correlations demonstrated
 158 the low persistence for both mentioned stations. According to the crisis of Lake Urmia, the amounts of
 159 precipitation and consequently river flow have decreased for the recent years; therefore, this may cause some
 160 difficulties in forecasting river flows.

161



162

163 **Fig. 4** Babarud and Vaniar stations, located at Lake Urmia basin <URL1>

164

165 **Table 1** Statistical parameters of the implemented data (X_{mean} , X_{max} , X_{min} , S_x , C_{sx} , a_1 , a_2 , a_3 denote the overall mean,
 166 maximum, minimum, standard deviation, skewness, lag -1, lag -2, lag -3 auto-correlation coefficients, respectively)

Station	Data set	X_{mean} (m^3/s)	X_{max} (m^3/s)	X_{min} (m^3/s)	S_x (m^3/s)	C_{sx} (m^3/s)	r_1	r_2	r_3
Babarud	Training data	8.75	66.50	0.00	9.63	2.05	0.70	0.25	-0.07
	Testing data	4.71	43.27	0.00	7.37	2.54	0.59	0.14	-0.12
	Entire data	7.74	66.50	0.00	9.28	2.13	0.69	0.25	-0.05
Vaniar	Training data	14.28	178.29	0.00	21.35	2.94	0.62	0.15	-0.11
	Testing data	5.66	65.30	0.00	10.50	3.02	0.50	0.11	-0.05
	Entire data	12.13	178.29	0.00	19.58	3.19	0.63	0.18	-0.07

167

168 4. Evaluation parameters

169 In this study, different evaluation parameters were considered for scrutinizing the precision of the mentioned
170 models for river flow forecasting.

171 As one of the widely-used statistical parameters, root mean squared error (RMSE) measures the average
172 amount of error (the difference between predicted and observed flows) appropriately, and it can be determined
173 as follows:

$$RMSE = \sqrt{\frac{1}{n} \sum_{i=1}^n (Q_p(i) - Q_o(i))^2} \quad (10)$$

174 where $Q_p(i)$, $Q_o(i)$, and n represent the predicted river flow, the observed river flow, and the number of
175 observations, respectively.

176 The bias in the predicted river flow is calculated by the mean absolute error (MAE) which measures the
177 closeness of the predictions to the actual flows. Lower MAE values represent more precise predictions of river
178 flow either equal or close to the observed values. It is calculated as follows:

$$MAE = \frac{1}{n} \sum_{i=1}^n |Q_p(i) - Q_o(i)| \quad (11)$$

179 The correlation coefficient (R), which describes the amount of linearity among simulated and observed values
180 of river flows, ranges from -1 to 1 and is described as follows:

$$R = \frac{\left(\sum_{i=1}^n Q_o(i) Q_p(i) - \frac{1}{n} \sum_{i=1}^n Q_o(i) \sum_{i=1}^n Q_p(i) \right)}{\sqrt{\left(\sum_{i=1}^n Q_o(i)^2 - \frac{1}{n} \left(\sum_{i=1}^n Q_o(i) \right)^2 \right) \left(\sum_{i=1}^n Q_p(i)^2 - \frac{1}{n} \left(\sum_{i=1}^n Q_p(i) \right)^2 \right)}} \quad (12)$$

181 Also, the Bayesian information criterion (BIC) was utilized to specify the best model parsimoniously which
182 means that the model with fewer input parameters could have better performance in comparison to others. BIC
183 measures models relative to each other; in fact, the model with the best performance has the smallest quantity
184 of the BIC (Burnham and Anderson, 2002). It is given as follows:

$$BIC = n * \ln\left(\frac{RSS}{n}\right) + K * \ln(n) \quad (13)$$

185 where K indicates the number of input parameters and RSS can be determined as follows:

$$RSS = \sum_{i=1}^n (Q_p(i) - Q_o(i))^2 \quad (14)$$

186 Furthermore, Taylor diagram (TD) which is a graphical illustration of the observed and forecasted data, was
 187 applied for inspecting the precision of models (Taylor, 2001). The TD has this capability to encapsulate some
 188 characteristics of the predicted and observed flows at the same time. This diagram can illustrate RMSE, R, and
 189 SD between the forecasted and actual data, simultaneously. In TD, the azimuth angle, the radial distance from
 190 the origin, and radial distance from the observed data point denote the R-value, the ratio of the normalized SD
 191 and the RMSE value of the prediction, respectively.

192

193 5. Results and discussion

194 For evaluating the effects of previous monthly flows, three input combinations were established. Moreover,
 195 the periodicity effect was inspected by appending a component π (1 to 12 for each month).

196

Table 2 Input parameters of the established models.

Model	Input parameters	Output parameters
1	Q_{t-1}	Q_t
2	Q_{t-1}, π	Q_t
3	Q_{t-1}, Q_{t-2}	Q_t
4	Q_{t-1}, Q_{t-2}, π	Q_t
5	$Q_{t-1}, Q_{t-2}, Q_{t-3}$	Q_t
6	$Q_{t-1}, Q_{t-2}, Q_{t-3}, \pi$	Q_t

197

198 The results of statistical parameters for studied techniques in the test phase for the Babarud station are given
 199 in Table 3. As mentioned before, π was appended to the input combinations 1,3, and 5 to examine the effect
 200 of periodicity. From the table, it is clear that the periodicity considerably increased each model's accuracy. For
 201 the FOASVR model, R increased from 0.63 (for input combination (1)) to 0.82 (for input combination (2)) and
 202 similarly, RMSE and MAE indices decreased from 5.74 to 4.36 and from 3.29 to 2.40, respectively. Regarding
 203 two previous cases, by adding periodicity component, R increased from 0.70 to 0.80 and RMSE, and MAE
 204 decreased from 5.33 to 4.50 and from 2.90 to 2.67, respectively. Finally, in the case of three previous
 205 discharges inputs, R increased from 0.67 to 0.79 and RMSE, and MAE decreased from 5.69 to 4.58 and from
 206 3.20 to 2.67, respectively. Comparison of FOASVR, M5, and SVR models indicated that the FOASVR-2

207 model whose inputs are Q_{t-1} , and π had better accuracy than the M5 and SVR models. M5 also performed better
208 than the SVR model. Overall, FOASVR performed better than SVR and M5s. Also, FOA increased the
209 accuracy of SVR by approximately 27% for RMSE and 38% for MAE in the second scenario which performed
210 roughly (4% RMSE and 14%MAE) better than M5. Without periodicity, FOASVR-3 indicated 6% better
211 performance than M5-3, and they performed better than the SVR-5 model. The relative RMSE and MAE
212 differences between the optimal FOASVR-3 model without periodicity and FOASVR-3 model with periodicity
213 input were 18.2% and 17.2%, respectively. From the BIC point of view FOASVR-2, M5-2, and SVR-4 with
214 the values of 597.55, 581.85, and 701.18 had better performance in comparison with other models which means
215 that these scenarios had parsimonious inputs (accurate result with fewer input parameters), respectively. So,
216 for this station input combination (2) was a reasonable choice. Time variation of observed and predicted river
217 flows by the optimal periodic and non-periodic FOASVR, M5 and SVR models are illustrated in Fig. 5 and 6.
218 It can be comprehended from the figures that all three periodic and non-periodic models considerably
219 underestimate some peak flows. It seems that preciseness of these models decreases with increasing flow rate.
220 However, the superior accuracy of FOASVR and M5 to the SVR model can be comprehended from these
221 figures. Comparison of Fig. 5 and 6 visibly indicate that the periodic models better approximates the observed
222 river flows than the non-periodic models. Fig. 9 displays the scattered diagrams of the observed and predicted
223 monthly river flows by each method. It is noticeably evident from the graphs that the SVR model performs
224 worse than the other two methods especially in the prediction of peak river flows. Comparison of two figures
225 reveals that the estimates of periodic models are more accurate than non-periodic models. Also, this figure
226 indicates that all models (periodic and non-periodic) overestimate some low flows.

227 The test statistics of the FOASVR, M5 and SVR models for the Vaniar station are also provided in Table 3.
228 Similarly, the encouraging influence of periodicity component on models' precision is clearly seen for this
229 station. For the FOASVR model, R increased from 0.57 (for input combination (1)) to 0.79 (for input
230 combination (2)) and similarly, RMSE and MAE values decreased from 8.78 to 6.58 and from 4.77 to 3.86,
231 respectively. In the case of two previous discharges inputs, by adding periodicity component, R increased from
232 0.55 to 0.80 and RMSE, and MAE decreased from 8.88 to 6.48 and from 4.97 to 3.75, respectively. Finally, in
233 the three previous discharges inputs case, R increased from 0.55 to 0.81 and RMSE, and MAE values decreased
234 from 8.99 to 6.33 and from 5.53 to 3.71, respectively. Comparison of three models revealed that the optimal
235 FOASVR-6 model whose inputs are Q_{t-1} , Q_{t-2} , Q_{t-3} , and π performed better than optimal M5-2 comprising Q_{t-1}

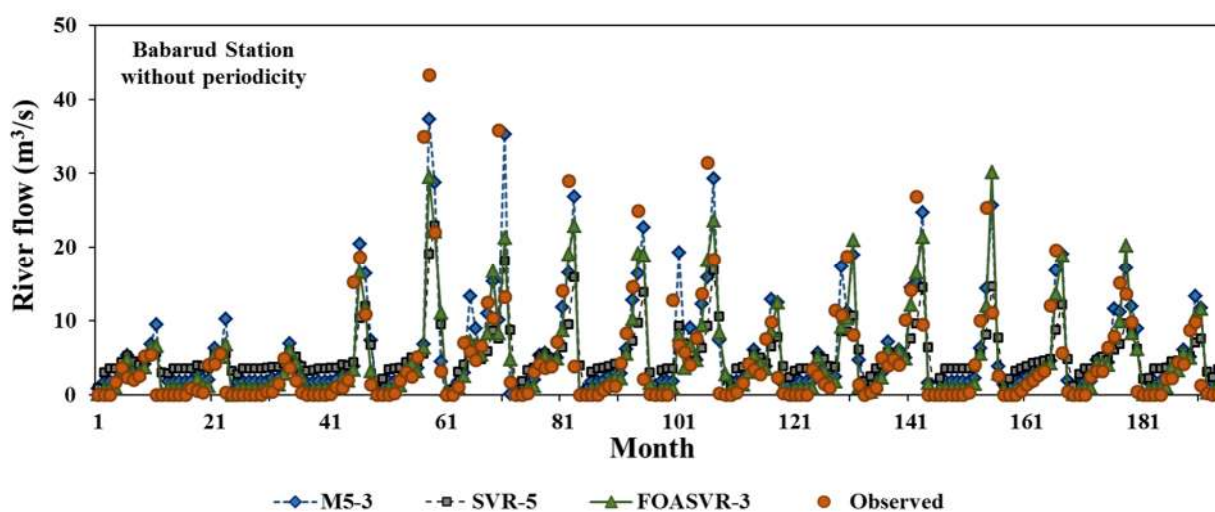
236 and π inputs and both performed better than the optimal SVR-6 model whose inputs are same as FOASVR-6.
 237 Generally, FOASVR performed better than SVR and M5 models, moreover, accuracy of SVR was increased
 238 by 29.7% and 30.4% related to RMSE and MAE in the optimal scenario (FOASVR-6) by applying FOA,
 239 respectively; also, FOASVR showed 16.8% and 19.7% better performances than M5 in terms of RMSE and
 240 MAE for this scenario, respectively. Without the periodicity component, the optimal FOASVR-1 model
 241 performed better than the optimal M5-1 and SVR-3 model. The relative RMSE and MAE differences between
 242 the optimal FOASVR-1 model without periodicity and FOASVR-1 model with periodicity input were 25.1%
 243 and 19.1%, respectively. The best values for BIC in this station were related to FOASVR-6 with 703.64, M5-
 244 2 with 740.34, and SVR-2 with 825.05. According to the fact that FOASVR-6 was closely followed by
 245 FOASVR-4 with the value of 707.09 and FOASVR-2 with the value of 707.53, it is better to choose a
 246 combination with fewer input parameters. Thus, the input parameters of Q_{t-1} and π were selected as a
 247 parsimonious scenario for this station similar to the previous station. Fig. 7 and 8 demonstrate the time variation
 248 of observed and predicted river flows by the optimal periodic and non-periodic FOASVR, M5 and SVR
 249 models. As found for the Vaniar station, here also the three periodic and non-periodic models underestimate
 250 some peak flows. Comparison of Fig. 7 and 8 confirm that appending the periodicity component as the input
 251 increases the estimation capacity of the models. The scatterplots of the observed and predicted monthly river
 252 flows by each method are shown in Fig. 9. Alike to the previous station, the FOASVR and M5 perform better
 253 than the SVR model especially in the prediction of peak river flows. This figure indicates that the estimates of
 254 periodic models are more accurate. According to Fig. 9, same as Babarud station, the models overestimate low
 255 flows in the Vaniar station, so, forecasting shifts from overestimation to underestimation with increasing flow
 256 rate.

257 **Table 3** The evaluation parameters of studied models in the test period

Model input	Model	Babarud Station				Vaniar Station			
		RMSE	MAE	R	BIC	RMSE	MAE	R	BIC
Q_{t-1}	SVR-1	6.10	4.10	0.59	706.88	9.33	5.60	0.50	831.52
	M5-1	5.94	3.62	0.61	696.57	9.57	5.44	0.54	840.91
	FOASVR-1	5.74	3.29	0.63	683.28	8.78	4.77	0.57	809.04
Q_{t-1}, π	SVR-2	5.97	3.88	0.61	703.79	9.04	5.31	0.52	825.05
	M5-2	4.54	2.73	0.80	597.55	7.19	4.46	0.77	740.34
	FOASVR-2	4.36	2.40	0.82	581.85	6.58	3.86	0.79	707.53
Q_{t-1}, Q_{t-2}	SVR-3	5.98	4.04	0.62	704.44	9.21	5.57	0.53	831.95
	M5-3	5.79	3.49	0.68	691.92	9.80	5.46	0.59	854.92

	FOASVR-3	5.33	2.90	0.70	659.80	8.88	4.97	0.55	818.45
Q_{t-1}, Q_{t-2}, π	SVR -4	5.85	3.83	0.64	701.18	8.96	5.33	0.54	826.99
	M5-4	4.55	2.83	0.80	603.67	7.58	4.64	0.76	765.10
	FOASVR-4	4.50	2.67	0.80	599.39	6.48	3.75	0.80	707.09
$Q_{t-1}, Q_{t-2}, Q_{t-3}$	SVR -5	5.91	3.90	0.62	705.14	9.22	5.73	0.52	837.57
	M5-5	5.79	3.50	0.68	697.18	9.79	5.55	0.60	859.76
	FOASVR-5	5.69	3.20	0.67	690.42	8.99	5.53	0.55	828.22
$Q_{t-1}, Q_{t-2}, Q_{t-3}, \pi$	SVR -6	5.82	3.77	0.64	704.46	9.01	5.53	0.53	834.27
	M5-6	4.54	2.84	0.80	608.09	7.61	4.62	0.75	771.78
	FOASVR-6	4.58	2.67	0.79	611.49	6.33	3.71	0.81	703.64

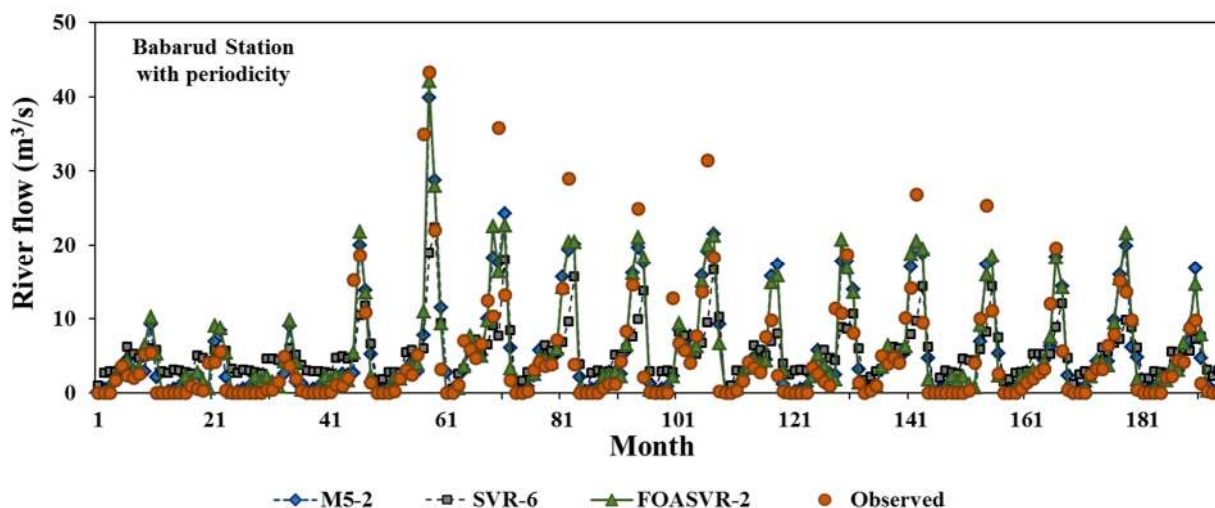
258



259

260

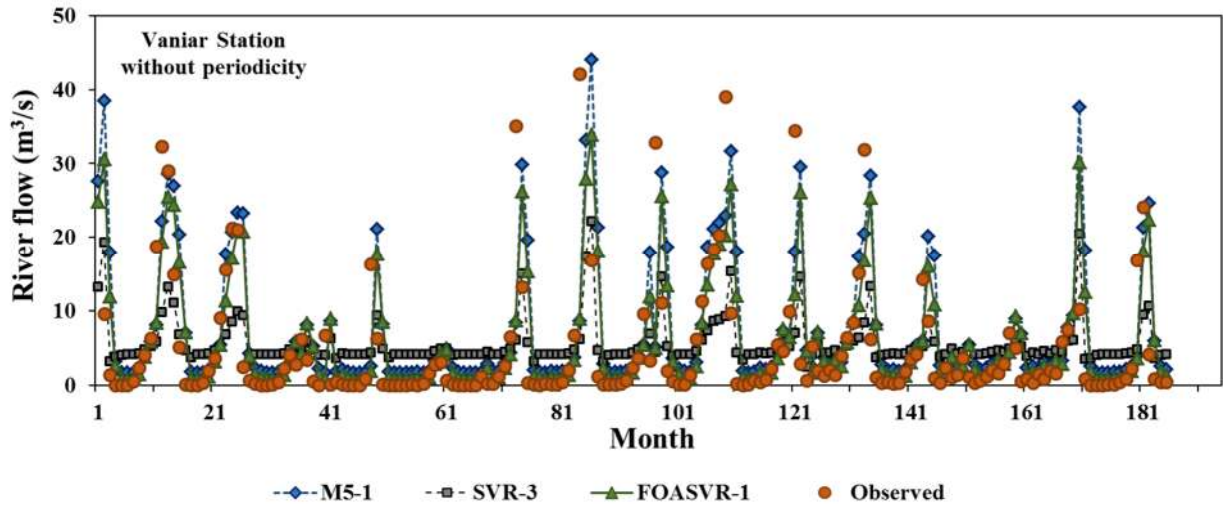
Fig. 5 The observed and forecasted monthly river flows without periodicity for Babarud station



261

262

Fig. 6 The observed and forecasted monthly river flows with periodicity for Babarud station

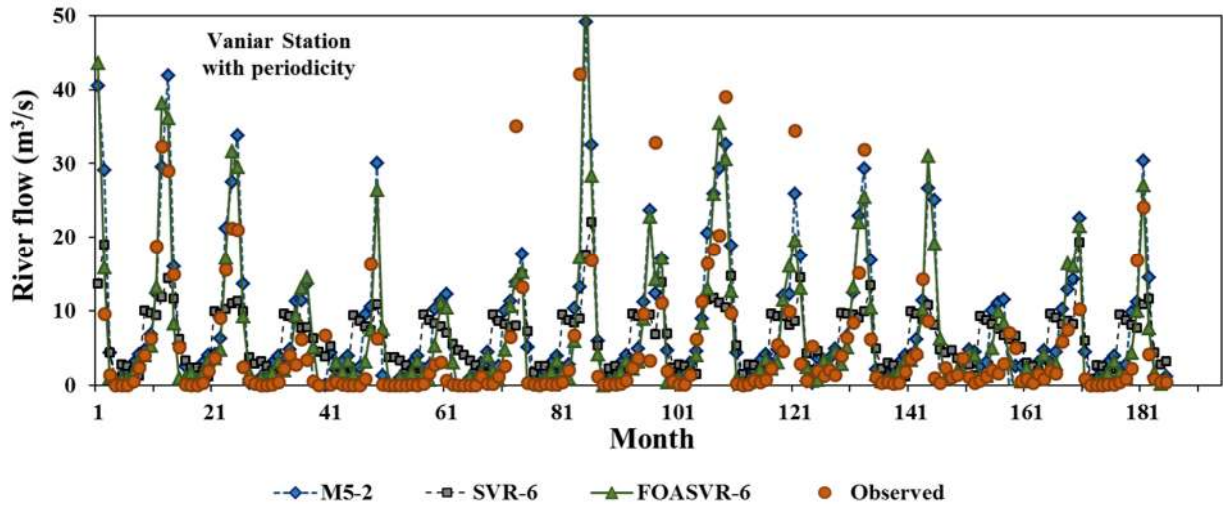


263

264

265

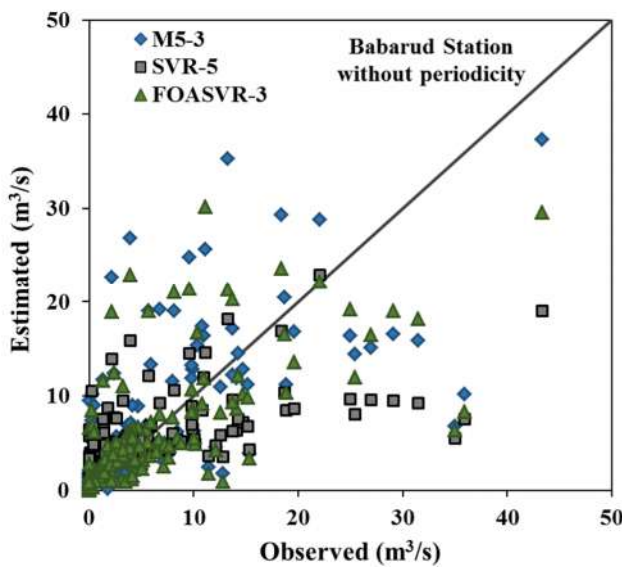
Fig. 7 The observed and forecasted monthly river flows without periodicity for Vaniar station



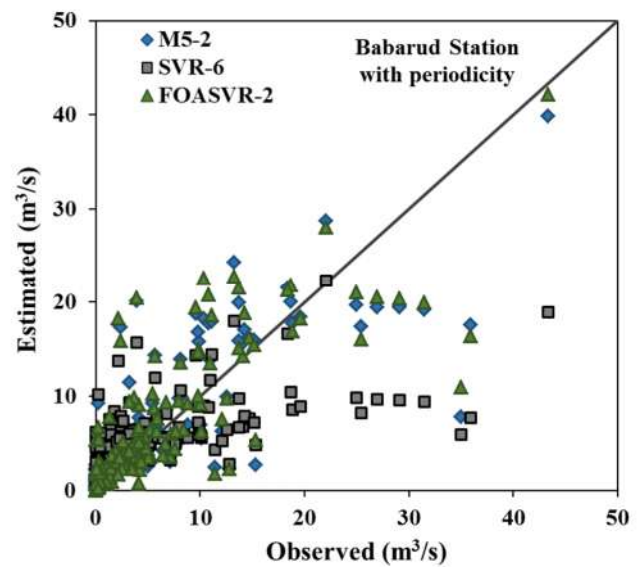
266

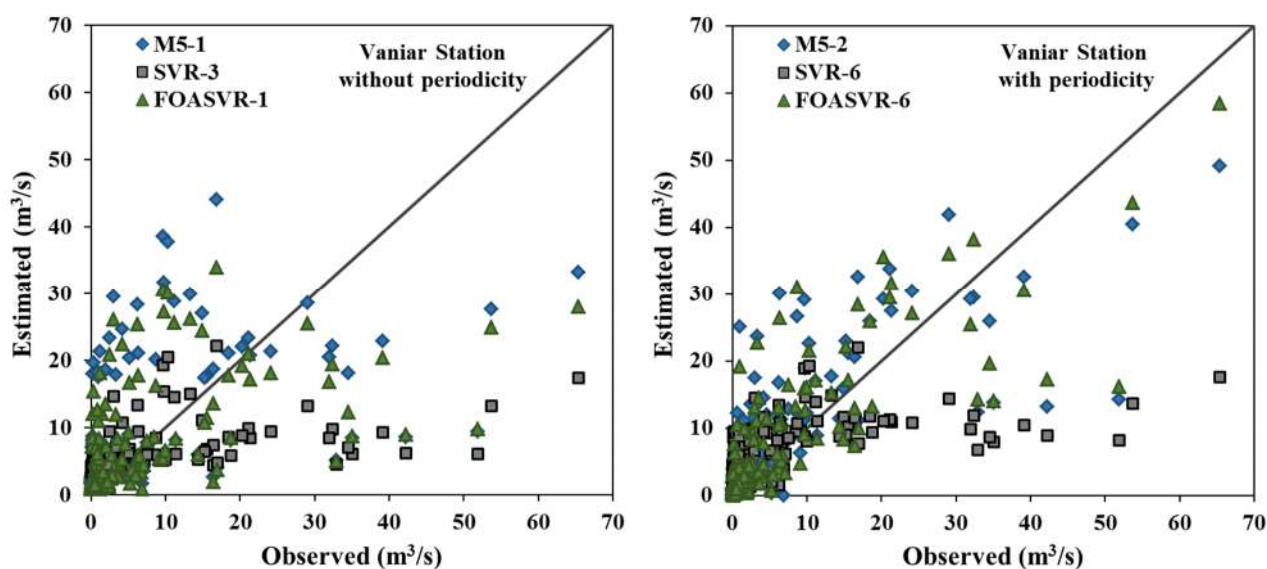
267

Fig. 8 The observed and forecasted monthly river flows with periodicity for Vaniar station



268





269

270 **Fig. 9** The scatterplots of observed and forecasted monthly river flows with and without periodicity for both stations

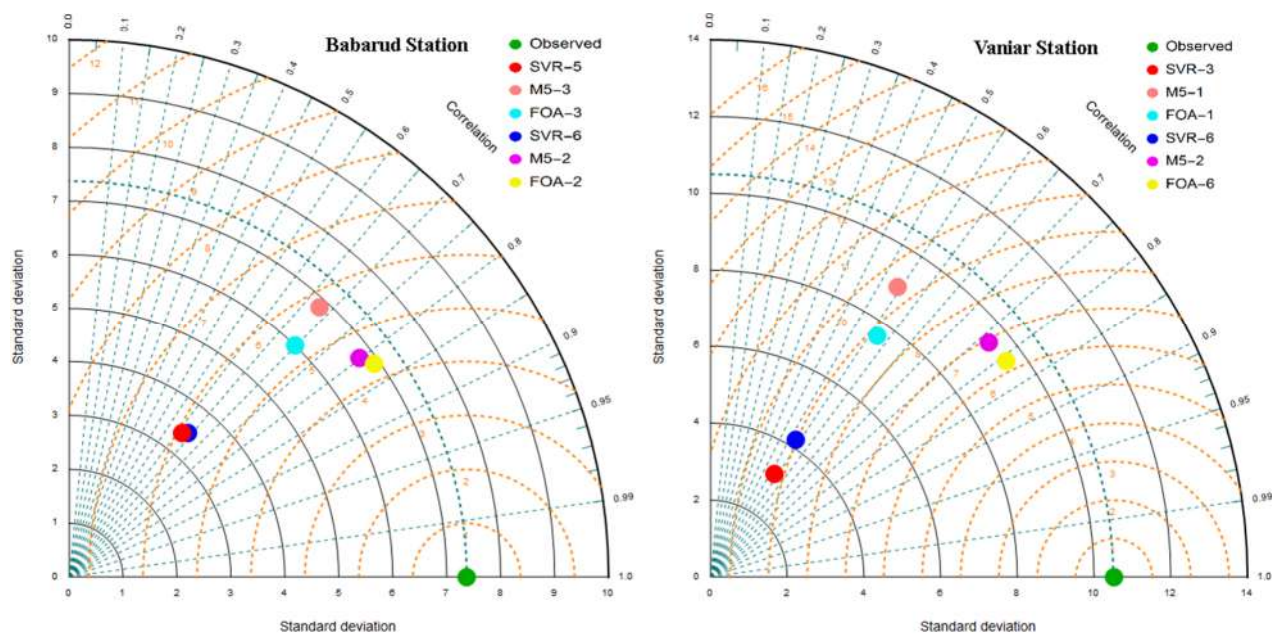
271

272 Furthermore, TDs were utilized for examining SD and R values for the FOASVR, M5 and SVR models. Fig.

273 10 exhibits TDs for all models, where the space from the reference green point is an amount of the centered

274 RMSE. So, it can be comprehended from Fig. 10 that FOASVR (a point with yellow color) provided relatively

275 precise predictions of river flow in both stations.



276

277

278 **Fig. 10.** TDs of the monthly predicted river flow

279

280

281 **6. Conclusion**

282 In the current study, three different data-driven techniques, FOASVR, M5, and SVR were compared in one
283 month ahead river flow forecasting in two stations, located in the Lake Urmia Basin of Iran. Comparison of
284 three periodic models specified that the periodic FOASVR model had better accuracy than the periodic M5
285 and SVR models. M5 was also found to achieve more suitable results than the SVR model. Similar to periodic
286 models, comparison of non-periodic models showed that the optimal FOASVR also had a better performance
287 than M5 and SVR models. It was proved that appending periodicity component significantly increases models'
288 accuracy in forecasting monthly river flows for both stations. For the Babarud station, the relative RMSE and
289 MAE differences between the optimal periodic and non-periodic FOASVR models were found to be 18.2%
290 and 17.2%, respectively. For the Vaniar station, the periodicity component decreased the RMSE and MAE
291 values of the optimal FOASVR models by 27.9 and 22.2%, respectively. According to BIC, the second input
292 combination (Q_{t-1} and π) opted as parsimonious inputs for FOASVR with values of 581.85 and 707.53 for
293 Babarud and Vaniar stations, respectively. Generally, the performance of FOASVR models was better than
294 the other two methods in forecasting monthly river flows. However, all methods indicated some difficulties in
295 forecasting river flow peaks while the FOASVR models provided a better forecast in high river flows.

296 **References**

- 297 Bhattacharya, B., Solomatine, D.P., 2005. Neural networks and M5 model trees in modeling water level–discharge
298 relationship. *Neurocomputing*. 63, 381–396.
- 299 Bhattacharya, B., Solomatine, D.P., 2006. Machine learning in sedimentation modeling. *Neural Networks*. 19, 208–214.
- 300 Burnham, K.P., Anderson, D.R., 2002. *Model Selection and Inference: a Practical Information-theoretic approach*, second
301 edition. Springer-Verlag, New York.
- 302 Cao, G., Wu, L., 2016. Support vector regression with fruit fly optimization algorithm for seasonal electricity consumption
303 forecasting. *Energy* 115, 734–745. doi:10.1016/j.energy.2016.09.065
- 304 Chang, C.-C., Lin, C.-J., 2001. Training ν -support vector classifiers: theory and algorithms. *Neural Comput.* 13(9), 2119–
305 47.
- 306 Cimen, M., 2008. Estimation of daily suspended sediments using support vector machines. *Hydrol. Sci. J.* 53 (3), 656–
307 666.
- 308 Esmailzadeh, B., Sattari, M.T., Samadianfard, S., 2017. Performance evaluation of ANNs and an M5 model tree in
309 Sattarkhan Reservoir inflow prediction. *ISH Journal of Hydraulic Engineering*. 1-10.

- 310 Fernando, A.K., Shamseldin, A.Y., Abrahart, B.J., 2012. River Flow Forecasting Using Gene Expression Programming
311 Models. 10th International Conference on Hydroinformatics HIC 2012. Hamburg, Germany.
- 312 Gunn, S.R., 1998. Support Vector Machines for Classification and Regression, Technical Report. University of
313 Southampton, England.
- 314 Ismail S., Samsudin, R., Shabri, A., 2010. River Flow Forecasting: a Hybrid Model of Self Organizing Maps and Least
315 Square Support Vector Machine. *Hydrol. Earth Syst. Sci. Discuss.* 7, 8179–8212.
- 316 Kalteh, A.M., 2013. Monthly river flow forecasting using artificial neural network and support vector regression models
317 coupled with wavelet transform. *Comput. Geosci.* 54, 1–8. doi:10.1016/j.cageo.2012.11.015
- 318 Khan, A.S., See, L., 2006. Rainfall-Runoff modeling using data-driven and statistical methods. Institute of Electrical and
319 Electronics Engineers (IEEE).
- 320 Lijuan, W., Guohua, C., 2016. Seasonal SVR with FOA algorithm for single-step and multi-step ahead forecasting in
321 monthly inbound tourist flow. *Knowledge-Based Syst.* 110, 157–166. doi:10.1016/j.knsys.2016.07.023
- 322 Liong, S.Y., Sivapragasam, C., 2002. Flood stage forecasting with support vector machines. *J. AWWRA.* 38 (1), 173–186.
- 323 Londhe, S.N., Dixit, P.R., 2011. Forecasting Stream Flow Using Model Trees. *International Journal of Earth Sciences
324 and Engineering.* 4(6), 282-285.
- 325 Londhe, S., Gavraskar, S.S., 2015. Forecasting One Day Ahead Stream Flow Using Support Vector Regression. *Aquat.
326 Procedia* 4, 900–907. doi:10.1016/j.aqpro.2015.02.113
- 327 Pan, W.-T., 2012. a new Fruit Fly Optimization Algorithm: Taking the financial distress model as an example.
328 *Knowledge-Based Syst.* 26, 69–74. doi:10.1016/j.knsys.2011.07.001
- 329 Onyari, E., Ilunga, F., 2010. Application of MLP neural network and M5P model tree in predicting streamflow: A case
330 study of Luvuvhu catchment, South Africa. *International Conference on Information and Multimedia Technology
331 (ICMT).* Hong Kong, China. V3, 156-160.
- 332 Quinlan, J.R., 1992. Learning with continuous classes. *Proceedings Fifth Australian Joint Conf. on Artificial Intelligence
333 (ed. by A. Adams & L. Sterling).* World Scientific, Singapore. 343–348.
- 334 Samadianfard, S., Nazemi, A.H., Sadraddini, A.A., 2014a. M5 model tree and gene expression programming based
335 modeling of sandy soil water movement under surface drip irrigation. *Agriculture Science Developments.* 3, 178-
336 190.
- 337 Samadianfard, S., Sattari, M.T., Kisi, O., Kazemi, H., 2014b. Determining flow friction factor in irrigation pipes using
338 data mining and artificial intelligence approaches. *Applied Artificial Intelligence.* 28, 793-813.
- 339 Sattari, M.T., Pal, M., Apaydin, H., Ozturk, F., 2013. M5 Model Tree Application in Daily River Flow Forecasting in
340 Sohu Stream, Turkey. *Water Resources.* 40(3), 233-242.

- 341 Siek, M., Solomatine, D.P., 2007. Tree-like machine learning models in hydrologic forecasting: optimality and expert
342 knowledge. *Geophysical Research Abstracts*. Vol. 9.
- 343 Smola, A.J., Scholkopf, B., 2004. A tutorial on support vector regression. *Statistics and Computing*. 14(3), 199-222.
- 344 Stravs, L., Brilly, M., 2007. Development of a low flow forecasting model using the M5 machine learning method.
345 *Hydrological Sciences*. 52(3), 466–477.
- 346 Taylor, K.E., 2001. Summarizing multiple aspects of model performance in a single diagram. *J. Geophys. Res. Atmos.*
347 106, 7183–7192.
- 348 <URL1><https://earth.google.com/web/@32.205151,53.07029487,2852.42968574a,2667368.97567809d,35y,0.1175398>
349 4h,16.72644158t,-0r
- 350 Vapnik, V., 1995. *The Nature of Statistical Learning Theory*. Springer Verlag, New York, USA.
- 351 Witten, I.H., Frank, E., 2005. *Data Mining: Practical Machine Learning Tools and Techniques with Java Implementations*.
352 Morgan Kaufmann: San Francisco.
- 353 Wu, C.L., Chau, K.W., Li, Y.S., 2008. River stage prediction based on a distributed support vector regression. *J.*
354 *Hydrol.* 358, 96–111. doi:10.1016/j.jhydrol.2008.05.028
- 355 Wu, C.-H., Tzeng, G.-H., Lin, R.-H., 2009. A Novel hybrid genetic algorithm for kernel function and parameter
356 optimization in support vector regression. *Expert Syst. Appl.* 36, 4725–4735. doi:10.1016/j.eswa.2008.06.046
- 357 Yu, X.Y., Liong, S.Y., Babovic, V., 2004. EC-SVM approach for realtime hydrologic forecasting. *J. Hydroinf.* 6 (3),
358 209–233.
- 359 Kurup, P.U., Dudani, N.K. Neural networks for profiling stress history of clays from PCPT data. *Journal of*
360 *Geotechnical and Geoenvironmental Engineering* 2014; 128(7): 569-579.
- 361 Samadianfard, S, Delirhasannia, R, Kisi, O, Agirre-Basurko, E. Comparative analysis of ozone level prediction models
362 using gene expression programming and multiple linear regression. *GEOFIZIKA* 2013; 30:43-74.
- 363 Samadianfard, S, Sattari, MT, Kisi, O, Kazemi, H. Determining flow friction factor in irrigation pipes using data mining
364 and artificial intelligence approaches. *Applied Artificial Intelligence* 2014; 28: 793-813.
- 365 Samadianfard, S., Asadi, E., Jarhan, S., Kazemi, H., Kheshtgar, S., Kisi, O., Sajjadi, S., Abdul Manaf, A., 2018.
366 Wavelet neural networks and gene expression programming models to predict short-term soil temperature at
367 different depths, *Soil and Tillage Research*, 175: 37-50.
- 368 Deo, R.C., Ghorbani, M.A., Samadianfard, S., Maraseni, T., Bilgili, M., & Biazar, M., 2018. Multi-layer perceptron
369 hybrid model integrated with the firefly optimizer algorithm for windspeed prediction of target site using a limited
370 set of neighboring reference station data, *Renewable Energy*, 116: 309-323.